

## Dynamics of a rotating beam with flexible root and flexible hub

A. A. Al-Qaisia<sup>†</sup>

*Mechanical Engineering Department, Faculty of Engineering and Technology  
University of Jordan, Amman 11942, JORDAN*

*(Received October 13, 2006, Accepted September 11, 2008)*

**Abstract.** A mathematical model for the nonlinear dynamics of a rotating beam with flexible root attached to a rotating hub with elastic foundation is developed. The model is developed based on the large planar and flexural deformation theory and the potential energy method to account for axial shortening due to bending deformation. In addition the exact nonlinear curvature is used in the system potential energy. The Lagrangian dynamics and the assumed mode method is used to derive the nonlinear coupled equations of motion hub rotation, beam tip deflection and hub horizontal and vertical displacements. The derived nonlinear model is simulated numerically and the results are presented and discussed for the effect of root flexibility, hub stiffness, torque type, torque period and excitation frequency and amplitude on the dynamic behavior of the rotating beam-hub and on its stability.

**Keywords :** rotating beam; flexible hub; flexible beam-root; non-linear dynamics; mathematical modelling.

---

### 1. Introduction

Mathematical modeling and dynamic analysis of rotating elastic structures has been the subject for many researchers and much research has been devoted to study the vibrations and dynamic analysis of such structures. A common particular interest of this engineering field is to understand its vibrational and dynamical behavior to help engineers in design, control, precise positioning, and performance evaluation in many applications such as: robotic manipulators, helicopter blades, turbomachinery blades and space applications.

The effect of attached masses and inertias, inclination angles, hub radius and beam length on natural frequencies and mode shapes have been studied thoroughly and a lot of investigations can be found in the open literature, also the problem of mathematical modeling and dynamic analysis of rotating beam-hub systems has attracted many researchers.

(Baruh and Tadikonda 1989) reported issues associated with modeling and control of robots with elastic arms. They showed that the centrifugal stiffening effect is the dominating factor for the system behavior; also they studied the effects of flexibility on the response and on the closed-loop control.

---

<sup>†</sup> Associate Professor, Ph.D., Corresponding author, E-mail: [alqaisia@ju.edu.jo](mailto:alqaisia@ju.edu.jo)

(Yigit *et al.* 1990) presented a model for the dynamics of a radially rotating beam with impact to predict the rigid body motion and the elastic motion before and after impact. The effect of axial shortening resulted from bending deformation and stiffening of the beam was considered in the governing equations. The presented model yielded nonlinear-coupled set of ordinary differential equations for the rigid body rotation and elastic deformation.

(Haering *et al.* 1994) developed a flexible body formulation called augmented imbedded geometric constraint for beam structures undergoing large overall motion. The formulation is problem independent and it is applicable to beam problems where the dominant stiffness effects are not known beforehand. (Tadikonda and Chang 1995) studied the effect of interbody forces on the flexible body dynamics in a multi-body chain undergoing large overall motions. (El-Absy and Shabana 1997) studied the effect of geometric stiffness forces on the stability of elastic and rigid body modes. The effect of longitudinal deformation due to bending is introduced to the dynamic equations using the principle of the virtual work method.

(Al-Bedoor and Hamdan 2001) developed a geometrically nonlinear model for a rotating flexible arm undergoing large planar flexural deformations. The effect of axial shortening due to bending deformation is included in the model. The developed model is simulated numerically and the effect of flexible arm length on the dynamic response is presented.

(Al-Qaisia 2004) extended the analysis (Al-Qaisia 2002), to study the nonlinear dynamic behavior of a rotating cantilever beam clamped with an attachment angle. Results were obtained and presented for the effect of: attachment angle; rotational speed; torque type; torque period; attached inertia element; and beam length on the dynamic behavior of the rotating beam-mass-hub.

(Al-Bedoor and Al-Qaisia 2002) studied the steady-state bending vibration and stability of a rotating blade, excited by shaft torsional vibrations using the harmonic balance method. Results were obtained analytically for small amplitude torsional excitations and compared with the numerical solutions. Also, they (Al-Bedoor and Al-Qaisia 2005), extended the analysis with no restrictions, neither on the strength of the torsional vibration nor on the torsional vibration excitation frequency to study the stability of bending vibration due to torsional excitations. The generalized method of harmonic balance is employed in finding the steady-state solutions in which the considered assumed solution contains integers and sub frequencies. The coefficient matrix eigenvalues of the steady-state solution are found for stability purposes. Stable and unstable regions as function of operational and design parameters are found and presented in map format. Numerical integration is used to check the predicted harmonic balance solution.

Recently, (Al-Qaisia and Al-Bedoor 2005) addressed the problem of rotating beams stiffening and developed different methods/models for accounting the rotating beam axial shortening due to bending deformations. In their study, they reported thorough analysis for the natural frequencies and fast Fourier Transform (FFT) of the system response and compared them with those obtained from four different models; (1) the potential energy model (PM), (2) kinetic energy model (KM), (3) kinetic and potential energy model (KPM), (4) Consistent model (CM) which does not account for the axial shortening. The potential energy model accounts for the axial shortening in the form of added elastic potential energy that results from the virtual work done by the centrifugal force, and the kinetic energy model includes the shortening effect in the velocity vector and the corresponding kinetic energy and finally the kinetic and potential energy model combines both approaches. Results of analysis showed that the approach that handles both the effect of rotating speed and the effect of vibration amplitude for all modes correctly is the potential energy model (PM).

The objective of this work is to study the dynamic response of a rotating beam with flexible root



## 2.2 Kinetic and potential energies

The global position vector of an arbitrary point  $P$ , in the  $XY$  inertial coordinates, Fig. 1, on the beam can be written as

$$R_p = \begin{pmatrix} X \\ Y \end{pmatrix} + R_H \begin{pmatrix} \cos \theta \\ \sin \theta \end{pmatrix} + [A(v')] [A(\theta)] r_p \quad (1)$$

where  $r_p$  is the position vector of the point  $P$  in the rotating body coordinate system  $xy$ ,  $A[(v')]$  is the rotational transformation matrix due to the flexibility of the rotational spring at the beam root,  $A[(\theta)]$  is the rotational transformation matrix from the body coordinate  $xy$  system to the inertial coordinates  $XY$ ,  $\theta$  is the hub rotation,  $R_H$  is the hub radius,  $X$  and  $Y$  are coordinates of the origin of rotating hub in the inertial coordinate  $XY$ .

The rotational transformation matrices, for the planar motion corresponding to the hub rotation  $A[(\theta)]$  and beam root flexibility  $A[(v')]$ , can be expressed respectively as

$$A[(\theta)] = \begin{bmatrix} \cos \theta & -\sin \theta \\ \sin \theta & \cos \theta \end{bmatrix} \quad (2)$$

$$A[(v')] = \begin{bmatrix} \cos v' & -\sin v' \\ \sin v' & \cos v' \end{bmatrix} \quad (3)$$

where  $v'$  is the slope of the beam transverse deflection at the root. It worth mentioning that the transformation matrix  $A[(v')]$ . Based on analysis conducted in this regard and for the same physical parameter of the beam-hub system considered in (Al-Qaisia 2004), and regardless the value of  $K_t$ , the calculated beam root flexibility transformation matrix  $A[(v')]$  is of the order

$$A[(v')] = \begin{bmatrix} 1 & 0 \\ 0 & 1 \end{bmatrix} \quad (4)$$

Consequently, and for all forthcoming formulation, the transformation matrix  $A[(v')]$  will not be considered in the mathematical modeling and the derivation of the governing equations of the system. Because it will have no effect neither on the qualitative nor on the quantitative dynamical behavior of the beam-hub system.

To develop the kinetic energy expression the velocity vector  $\dot{R}_p$  can be represented as follows

$$\dot{R}_p = \begin{pmatrix} \dot{X} \\ \dot{Y} \end{pmatrix} + \dot{\theta} R_H \begin{pmatrix} -\sin \theta \\ \cos \theta \end{pmatrix} + [A(\theta)] \dot{r}_p + [A_\theta(\theta)] r_p \quad (5)$$

where  $A_\theta(\theta) = [dA/d\theta]$ ,  $r_p = si + vj$  and  $\dot{r}_p = \dot{v}j$ .

Now the kinetic energy of the beam-mass-hub system under consideration can be expressed as

$$KE = \frac{1}{2} m_b \int_0^1 \dot{R}_p^T \cdot \dot{R}_p d\zeta + \frac{1}{2} \{ I_H \dot{\theta}^2 + m_H (\dot{X}^2 + \dot{Y}^2) \} \quad (6)$$

where  $m_b = \rho l$  is the constant mass of the beam,  $\zeta = s/l$  is dimensionless position of the material point,  $I_H$  is the mass moment of inertia of the hub ( $I_H = m_H R_H^2 / 2$ ) and  $m_H$  is the mass of the hub.

Upon substituting for  $r_p$ ,  $\dot{r}_p$ ,  $[A(\theta)]$  and  $[A_\theta(\theta)]$  into Eq. (6), the kinetic energy of the considered system takes the form

$$KE = \frac{m_b}{2} \left\{ \int_0^1 \dot{R}_p^2 d\zeta + \frac{I_H}{m_b} \dot{\theta}^2 + \frac{m_H}{m_b} (\dot{X}^2 + \dot{Y}^2) \right\} \quad (7)$$

where  $\dot{R}_p^2$  is given by

$$\begin{aligned} \dot{R}_p^2 = & \dot{X}^2 + \dot{Y}^2 + \{ \dot{\theta}^2 [R_H + s]^2 + \dot{\theta}^2 v^2 + 2 \dot{\theta} \dot{v} [R_H + s] + \dot{v}^2 \} \\ & + 2 \cos \theta \{ \dot{\theta} [R_H + s] \dot{Y} - v \dot{X} \} + \dot{v} \dot{Y} - 2 \sin \theta \{ \dot{\theta} [R_H + s] \dot{X} + v \dot{Y} \} + \dot{v} \dot{X} \end{aligned} \quad (8)$$

The system potential energy is constituted from; the elastic beam strain energy  $V_E$ , the potential energies stored in the rotational springs  $V_S$  at the beam root  $K_t$  and the two linear springs attached to the hub in the vertical and horizontal directions  $K_x$  and  $K_y$ , and the potential energy  $V_A$  of the axial shortening  $u$  “see Fig. 1b” due to transverse deformation and the generated inertial force.

The elastic beam nonlinear strain energy for the beam due to nonlinear curvature is given by

$$V_E = \frac{EI\lambda^3}{2} \int_0^1 (v''^2 + \lambda^2 v''^2 v'^2) d\zeta \quad (9)$$

where  $\lambda = 1/l$ , and  $v$  is the beam bending deflection

The elastic potential energy stored in the springs is given by

$$V_s = \frac{1}{2} \{ K_t v'^2 + K_x X^2 + K_y Y^2 \} \quad (10)$$

The inertial force on the material point  $P$  of the beam results from the rotational motion can be expressed in the form

$$F_p = \int_{\zeta}^l \rho (R_H + l\zeta) \dot{\theta}^2 l d\zeta = \rho l^2 \dot{\theta}^2 \int_{\zeta}^l \left( \frac{R_H}{l} + \zeta \right) d\zeta \quad (11)$$

Upon evaluating the integral given in Eq. (11), the inertial force is given by

$$F_p = \rho l^2 \dot{\theta}^2 \left[ \frac{R_H}{l} (1 - \zeta) + \frac{1}{2} (1 - \zeta^2) \right] \quad (12)$$

The virtual work that results from the axial shortening  $u$  under the effect of the inertial forces of Eq. (12) can be called the axial shortening potential energy  $V_A$  and can be written as

$$V_A = \int_0^1 F_p \cdot du \quad (13)$$

The axial shortening  $u$  due to the flexural bending  $v$  of the beam can be derived by imposing the inextensibility condition which has been used in previous studies (Al-Bedoor and Hamdan 2001, Al-Qaisia 2004) allows one to relate, through a consistent geometric consideration, axial displacement (shortening)  $u$  due to the flexural bending  $v$

$$u = \frac{1}{2} \int_0^{\zeta} \left( \lambda v'^2 + \frac{\lambda^3}{4} v'^4 \right) d\zeta \quad (14)$$

Substituting the inertial force  $F_p$  (12) and the axial shortening  $u$  (14) into the integral of Eq. (13) yields

$$V_A = \frac{-\rho l^2 \dot{\theta}^2}{2\lambda} \int_0^1 \left\{ \frac{R_H}{l} (1 - \zeta) + \frac{1}{2} (1 - \zeta^2) \right\} \left( \lambda^2 v'^2 + \frac{\lambda^4}{4} v'^4 \right) d\zeta \quad (15)$$

Now the system potential energy becomes

$$PE = V_E + V_3 + V_A \quad (16)$$

### 2.3. Assumed mode method

Using Eqs. (17) and (18) for the kinetic and potential energies respectively, and as one can see the system energies is a function of the transverse deflection only,  $v$  and  $\dot{v}$ , the Lagrangian of the system  $L$  can be obtained as

$$L = KE - PE \quad (17)$$

The Lagrangian of the system  $L$  ( $L = KE - PE$ ) can be discretized by using the assumed mode method and substituting  $v(\zeta, t) = \sum_{i=1}^N \phi_i(\zeta)q_i(t)$  in the system Lagrangian.

where  $\phi_i(\zeta)$  is the normalized, self-similar assumed mode shape of the beam-mass and  $q(t)$  is an unknown time modulation of the assumed deflection mode  $\phi_i(\zeta)$ . In the present work the beam-mass mode shape  $\phi_i(\zeta)$  is assumed to be that of the non-rotating linear beam which can be written in the form

$$\phi_i(\zeta) = A \sin p_i \zeta + B \cos p_i \zeta + C \sin p_i \zeta + D \cosh p_i \zeta \quad (18)$$

where  $A$ ,  $B$ ,  $C$  and  $D$  are arbitrary constants to be determined by using the following four boundary conditions

$$\phi_i(0) = 0, \quad \phi_i''(1) = 0, \quad \phi_i'''(1) = 0 \quad \text{and} \quad \phi_i''(0) - S_i \phi_i'(0) = 0$$

where  $S_i = K_i l / EI$ .

### 2.4. Equations of motion

Using the expression of the kinetic energy, potential energies of the beam-hub system and the assumed mode method the Lagrangian  $L$ , can be written in the form

$$\begin{aligned} L = & \frac{m_B l^2}{2} \{ \beta_1 \dot{\theta}^2 + \beta_2 \dot{\theta}^2 q^2 + \beta_3 \dot{\theta} \dot{q} + \beta_4 \dot{q}^2 - \beta^2 \beta_5 q^2 - \beta^2 \beta_6 q^4 - \beta_7 \dot{\theta}^2 q^2 - \beta_8 \dot{\theta}^2 q^4 \} \\ & + \cos \theta [ \dot{\theta} (\beta_9 \dot{y} - \beta_{10} q \dot{x} + \beta_{11} \dot{y}) + \beta_{12} \dot{q} \dot{y} ] - \sin \theta [ \dot{\theta} (\beta_9 \dot{x} + \beta_{10} q \dot{y} + \beta_{11} \dot{x}) + \beta_{12} \dot{q} \dot{x} ] \\ & + \dot{x}^2 + \dot{y}^2 + \beta_{13} (\dot{x}^2 + \dot{y}^2) - \beta^2 (s_x x^2 + s_y y^2) - \beta^2 s_i (\beta_{14} q^2 + \beta_{15} q^4) \end{aligned} \quad (19)$$

where

$$\beta^2 = \frac{EI \lambda^4}{\rho}, \quad x = X/l, \quad y = Y/l$$

$$\beta_1 = a_1 + \frac{1}{3} + \frac{R_H}{l} + \left( \frac{R_H}{l} \right)^2, \quad a_1 = \frac{m_H}{m_b}$$

$$\beta_2 = \int_0^1 \phi^2 d\zeta$$

$$\beta_3 = 2 \int_0^1 \phi \left( \zeta + \frac{R_H}{l} \right) d\zeta$$

$$\begin{aligned}
\beta_4 &= \int_0^1 \phi^2 d\zeta \\
\beta_5 &= \int_0^1 \phi'^2 d\zeta \\
\beta_6 &= \int_0^1 \phi'^2 \phi'^2 d\zeta \\
\beta_7 &= -\int_0^1 \phi^2 \left( \frac{R_H}{l} + \frac{1}{2} - \zeta - \frac{\zeta^2}{2} \right) d\zeta \\
\beta_8 &= \frac{-l}{4} \int_0^1 \phi'^4 \left( \frac{R_H}{l} + \frac{1}{2} - \zeta - \frac{\zeta^2}{2} \right) d\zeta \\
\beta_9 &= 2 \int_0^1 \frac{R_H}{l} d\zeta = \frac{2R_H}{l} \\
\beta_{10} &= 2 \int_0^1 \phi d\zeta \\
\beta_{11} &= 2 \int_0^1 \zeta d\zeta = 1 \\
\beta_{12} &= 2 \int_0^1 \phi d\zeta \\
\beta_{13} &= \frac{m_H}{m_b} \\
\beta_{14} &= \phi'^2 \Big|_{\zeta=0} \\
\beta_{15} &= \frac{\phi'^4}{3} \Big|_{\zeta=0} \\
S_x &= \frac{K_x l^3}{EI} \\
S_y &= \frac{K_y l^3}{EI} \\
S_t &= \frac{K_t l}{EI}
\end{aligned} \tag{20}$$

Using the virtual work method, the external torque  $T$  applied at the hub can be represented in the form:

$$\delta W = T \delta \theta \tag{21}$$

Applying Euler-Lagrangian method, the system equations of motion are obtained for  $\theta$ ,  $q$ ,  $x$  and  $y$  as follows

$$\begin{aligned}
& 2[\beta_1 + (\beta_2 - \beta_7)q^2 - \beta_8 q^4] \ddot{\theta} + 4(\beta_2 - \beta_7) \dot{\theta} q \dot{q} - 8\beta_8 \dot{\theta} q^3 \dot{q} + \beta_3 \ddot{q} \\
& - [\beta_{10} q \cos \theta + (\beta_9 + \beta_{11}) \sin \theta] \ddot{x} + [(\beta_9 + \beta_{11}) \cos \theta - \beta_{10} q \sin \theta] \ddot{y} = \frac{2T}{m_B l^2}
\end{aligned} \tag{22}$$

$$2\beta_4\ddot{q} + 2[\beta^2\beta_5 + (\beta_7 - \beta_2)\dot{\theta}^2 + \beta^2\beta_{14}S_1]q + 4[\beta^2\beta_6 + \beta_8\dot{\theta}^2 + \beta^2\beta_{15}S_1]q^3 + \beta_3\ddot{\theta} + \beta_{12}(\cos\theta\ddot{y} - \sin\theta\ddot{x}) = 0 \quad (23)$$

$$[2 + 2\beta_{13}]\ddot{x} + 2\beta^2S_x x - [\beta_{10}q\cos\theta + (\beta_9 + \beta_{11})\sin\theta]\ddot{\theta} - \beta_{12}\sin\theta\ddot{q} - \cos\theta(\beta_{10} + \beta_{12})\dot{q}\dot{\theta} + [\beta_{10}q\sin\theta - (\beta_9 + \beta_{11})\cos\theta]\dot{\theta}^2 = 0 \quad (24)$$

$$[2 + 2\beta_{13}]\ddot{y} + 2\beta^2S_y y + [(\beta_9 + \beta_{11})\cos\theta - \beta_{10}q\sin\theta]\ddot{\theta} + \beta_{12}\cos\theta\ddot{q} - \sin\theta(\beta_{10} + \beta_{12})\dot{q}\dot{\theta} - [\beta_{10}q\cos\theta + (\beta_9 + \beta_{11})\sin\theta]\dot{\theta}^2 = 0 \quad (25)$$

Eqs. (22-25) represent the system mathematical model, which consists of four nonlinear-coupled differential equation for the four degrees of freedom. The first equation represents the rigid body motion  $\theta$ , the second represents the elastic deflection of the beam  $q$  and the third and fourth equations represent the horizontal and vertical motion of the hub  $x$  and  $y$ , respectively.

By examining the equations of motions of the flexible beam-hub system, one can note the presence of nonlinear terms due to; the curvature  $q^3$ , inertia  $q^2\dot{\theta}$  and  $q^4\ddot{\theta}$ , coriolis acceleration  $q^3\dot{\theta}\dot{q}$  and other terms. These terms will have a dominant role in the dynamic behavior of the system due to the interaction between the degrees of freedom of the system, as one can see from the simulation results of the dynamic response of the beam-hub in the next section.

### 3. Results and discussion

The nonlinear response of the rotating beam-hub system, was calculated numerically by solving the coupled nonlinear differential equations of motion (22-25), for various values of physical parameters  $K_t$ ,  $K_x$ ,  $K_y$  and external torque  $T$ , using a variable step predictor-corrector algorithm "MATLAB software". The system parameters  $\beta_i$ ,  $i=1, \dots, 15$  given in Eq. (20) are evaluated numerically.

The physical properties of the beam and hub were chosen to be the same properties considered in (Al-Qaisia 2003, Al-Qaisia 2004) which are given in Table 1.

To calculate the nonlinear response of the rotating beam-hub system, the inverse dynamics was used to design an open-loop maneuver, which is similar to the procedure used in (Al-Qaisia 2004), which accounts for the rigid body rotation, such that,  $\theta(0) = 0$  and  $\theta(\tau) = \theta_\tau$ , where  $\tau$  is the time of the maneuver and  $\theta_\tau$  is the target position. Here, also and for the sake of comparison, two torque profiles are used, linear and sinusoidal, and they are given, respectively, by Eqs. (26) and (27)

Table 1 Beam-Hub properties

Property	Value
Beam length, $L$	2.0 m
Beam flexural rigidity, $EI$	756.65 N m <sup>2</sup>
Beam mass per unit length, $\rho$	4.015 kg/m
Hub radius, $R_H$	0.2 m
Hub mass, $M_H$	50.0 kg

$$\left\{ \begin{array}{l} T(t) = \frac{24J_{tot}\theta_\tau}{\tau}t, \quad 0 \leq t \leq \tau/2 \\ T(t) = \frac{24J_{tot}\theta_\tau}{\tau^3}(t-\tau), \quad \tau/2 \leq t \leq \tau \\ T(t) = 0, \quad t > \tau \end{array} \right\} \quad (26)$$

$$\left\{ \begin{array}{l} T(t) = \frac{2\pi J_{tot}\theta_\tau}{\tau^2} \sin\left(\frac{2\pi t}{\tau}\right), \quad 0 \leq t \leq \tau \\ T(t) = 0, \quad t > \tau \end{array} \right\} \quad (27)$$

where  $J_{tot}$  is the total mass moment of inertia of the system. Figs. (2-4) shows the two types of torque profiles that are used to rotate the system an angle of  $\theta_\tau = 30^\circ (\pi/6)$ ,  $\tau = 2s$  and the corresponding angular positions and velocities. The nonlinear dynamic behavior of the beam-hub system was first simulated for relatively high values of  $K_t = K_x = K_y = 10^6$  and for two types of torque profiles. For the linear torque, the beam tip deflection of the first mode is shown in Fig. 5, the angular position of the hub is shown in Fig. 6 and the corresponding deflections of the hub in  $x$  and  $y$  directions are shown in Figs. 7 and 8, respectively. Same results were obtained for the system but for a sinusoidal torque and presented in Figs. 9-12. It is clear that for the sinusoidal torque, the nonlinear response of the system is smooth and the hub reaches its prescribed target position  $\theta_\tau = 30^\circ (\pi/6)$ , on the other hand for the linear torque, the hub reaches the target position but with some damping effects and this due to the presence of nonlinear interaction between the degrees of freedom of the system,  $(\theta, q, x \text{ and } y)$ , and consequently some of the energy fed to the system is transferred from one degree to another.

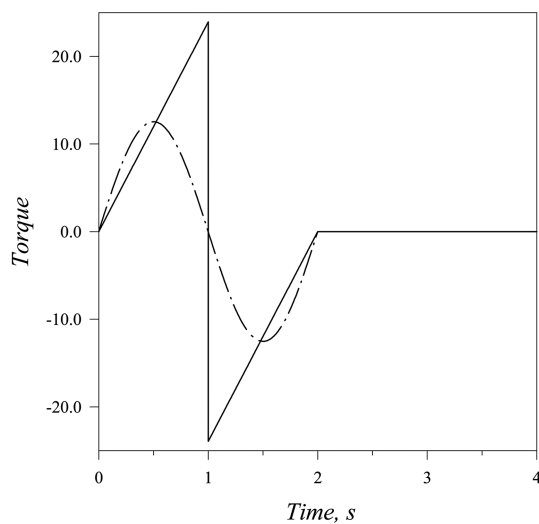


Fig. 2 Torque profiles used to rotate the system  $30^\circ (\pi/6)$  in 2 sec  
 — linear torque profile, — · — sinusoidal torque profile

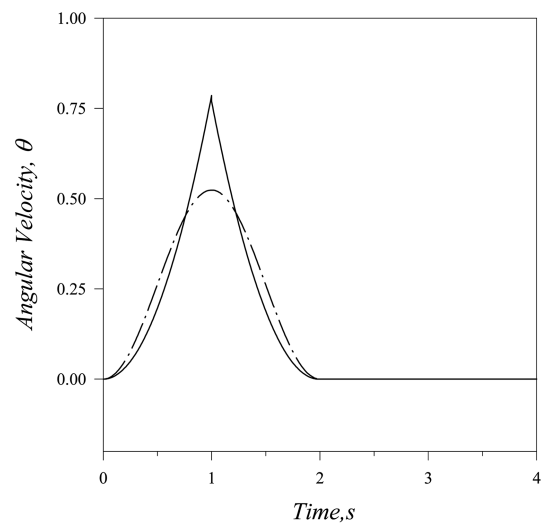


Fig. 3 Angular velocities corresponding to — linear and — · — sinusoidal torque profiles

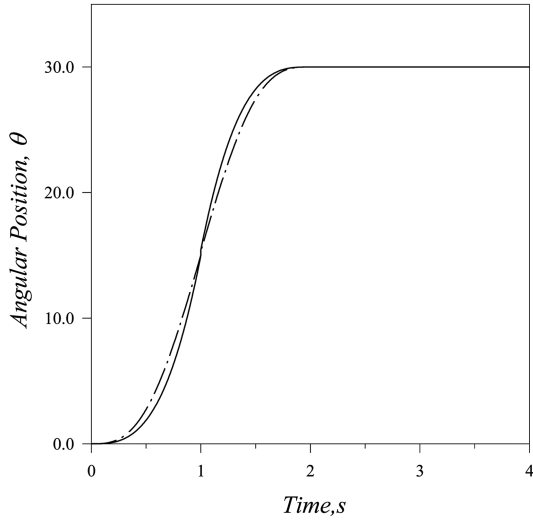


Fig. 4 Angular positions corresponding to — linear and — · — sinusoidal torque profiles

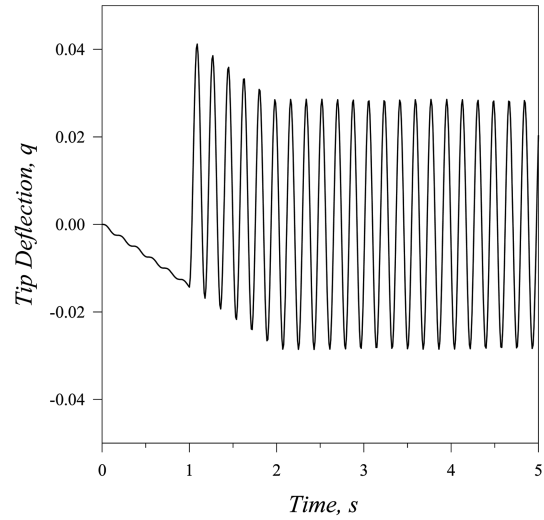


Fig. 5 Beam tip deflection for  $K_t = K_x = K_y = 10^6$   $N/m$  and linear torque profile,  $\theta_\tau = \pi/6$  and  $\tau = 2$  sec

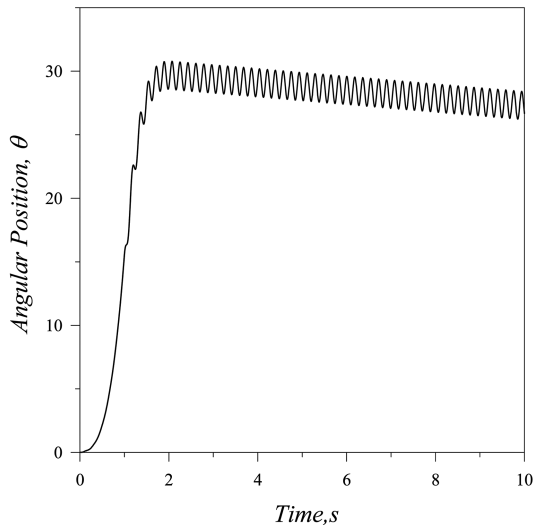


Fig. 6 Hub angular position for  $K_t = K_x = K_y = 10^6$   $N/m$  and linear torque profile and  $\theta_\tau = \pi/6$  and  $\tau = 2$  sec

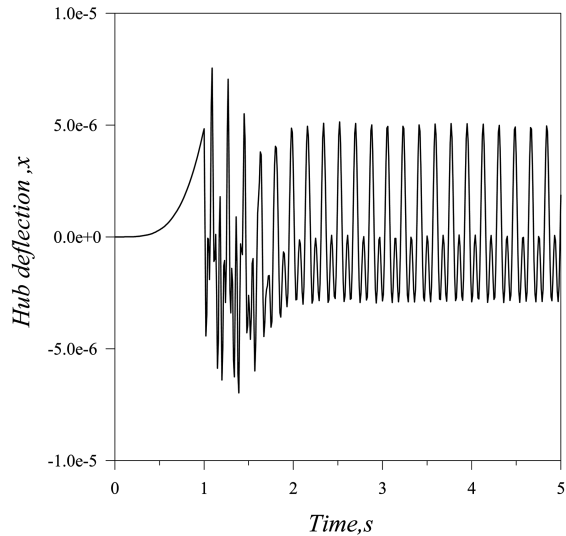


Fig. 7 Horizontal Hub displacement  $x$  for  $K_t = K_x = K_y = 10^6$   $N/m$  and linear torque profile and  $\theta_\tau = \pi/6$  and  $\tau = 2$  sec

The nonlinear response of the beam-hub system is studied and simulations results were obtained for different values of  $K_t, K_x, K_y$ , torque profiles, maneuver time  $\tau$  and for different modes of the beam.

In Figs. 13 and 14, the hub angular position  $\theta$  and  $x$  deflection are shown respectively for  $K_t = 10^7, K_x = 10^3, K_y = 10^3$  and linear torque profile with  $\tau = 2s$ . The response exhibits a beating phenomenon in both Figures and this due to the fact that, the frequency of the input torque, i.e.  $(1/\tau)$ , is very

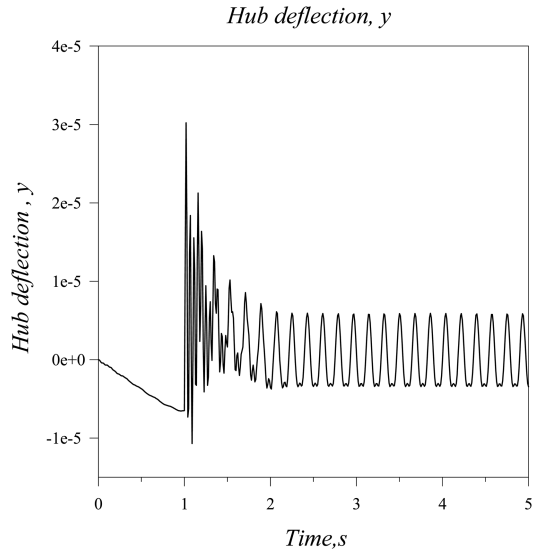


Fig. 8 Vertical Hub displacement  $y$  for  $K_t = K_x = K_y = 10^6$  N/m and linear torque profile and  $\theta_r = \pi/6$  and  $\tau = 2$   $\tau = 2$  sec

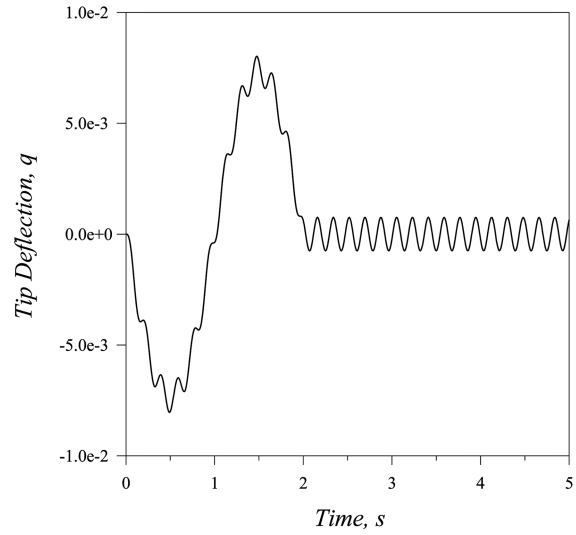


Fig. 9 Beam tip deflection for  $K_t = K_x = K_y = 10^6$  N/m and sinusoidal torque profile,  $\theta_r = \pi/6$  and  $\tau = 2$   $\tau = 2$  sec

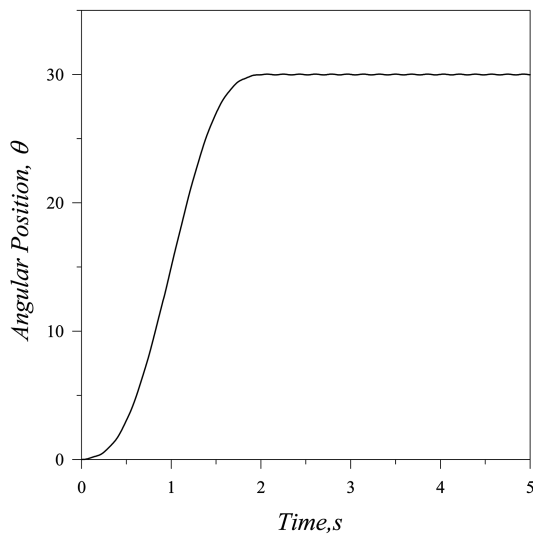


Fig. 10 Hub angular position for  $K_t = K_x = K_y = 10^6$  N/m and sinusoidal torque profile and  $\theta_r = \pi/6$  and  $\tau = 2$   $\tau = 2$  sec

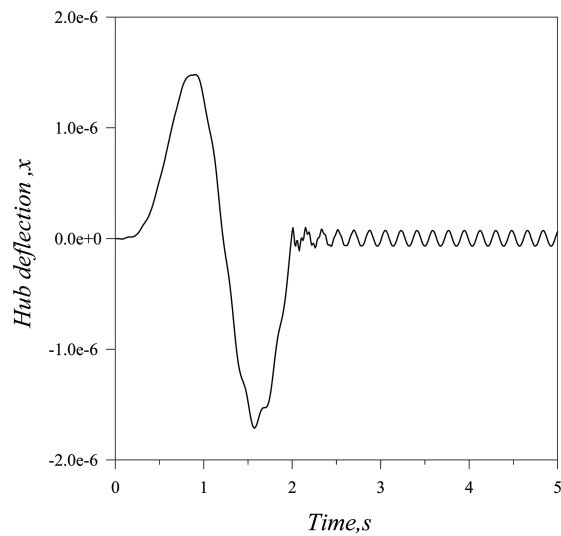


Fig. 11 Horizontal Hub displacement  $x$  for  $K_t = K_x = K_y = 10^6$  N/m and sinusoidal torque profile and  $\theta_r = \pi/6$  and  $\tau = 2$   $\tau = 2$  sec

close to the first natural frequency of the system.

The system is then simulated but for  $K_t = 10^6$ ,  $K_x = 10^4$  and  $K_y = 10^3$ , as shown in Fig. 15, the hub reaches its target position at the end of maneuver period but it continue to increase by time. Other results, but not shown, for the hub deflections and beam tip deflation indicate that this case is

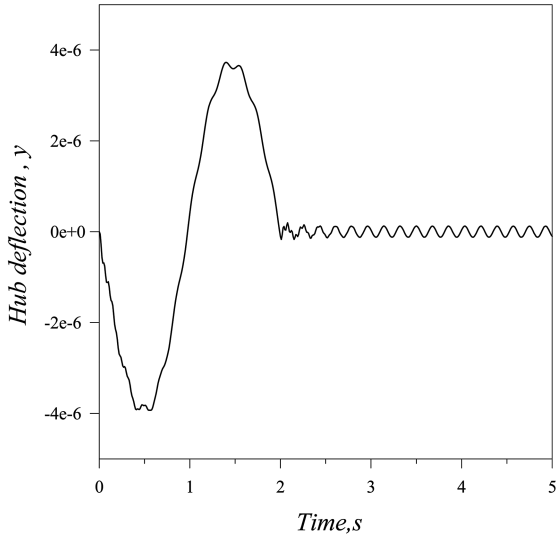


Fig. 12 Vertical Hub displacement  $y$  for  $K_t = K_x = K_y = 10^6 \text{ N/m}$  and sinusoidal torque profile and  $\theta_r = \pi/6$  and  $\tau = 2 \text{ sec}$

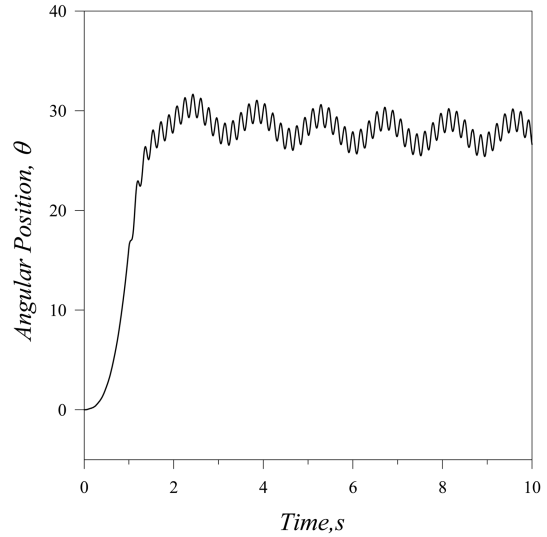


Fig. 13 Hub angular position for  $K_t = 10^7, K_x = K_y = 10^3 \text{ N/m}$  and linear torque profile

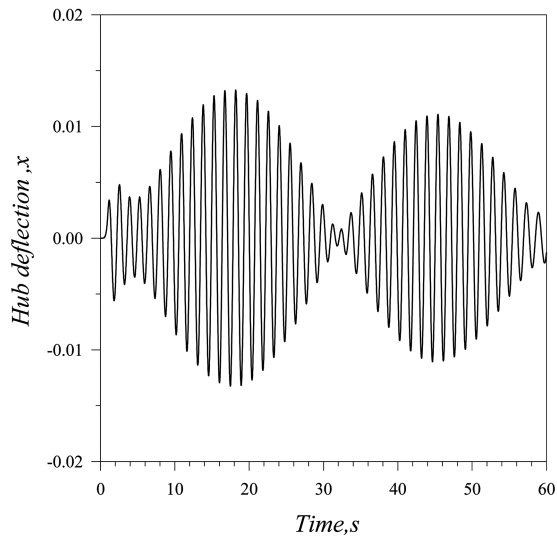


Fig. 14 Horizontal Hub deflection  $x$  for  $K_t = 10^7, K_x = K_y = 10^3 \text{ N/m}$  and linear torque profile

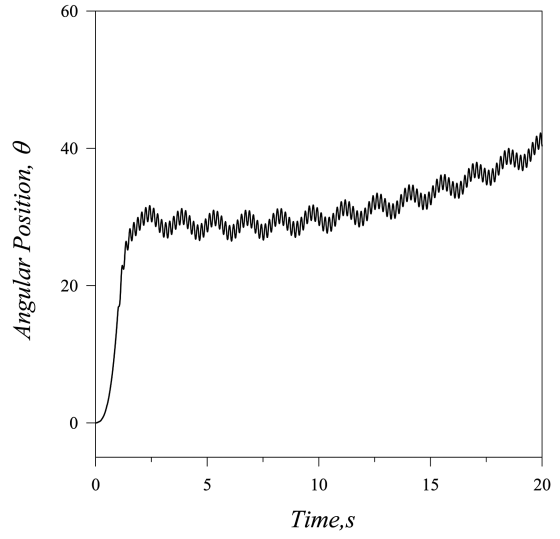


Fig. 15 Hub angular position for  $K_t = 10^6, K_x = 10^4, K_y = 10^3 \text{ N/m}$  and linear torque profile

resonance and the system becomes unstable due to the high amplitude of the hub deflections and due to the build up in the angular position magnitude.

Other simulations but for different values  $K_t, K_x, K_y$ , are shown in Figs. 16 and 17, in which the hub deflection in the  $x$  direction show a beating phenomenon, which is similar to the case presented previously in Figs. 13 and 14, at which the amplitude of the of motion builds up and then diminishes in a regular pattern.

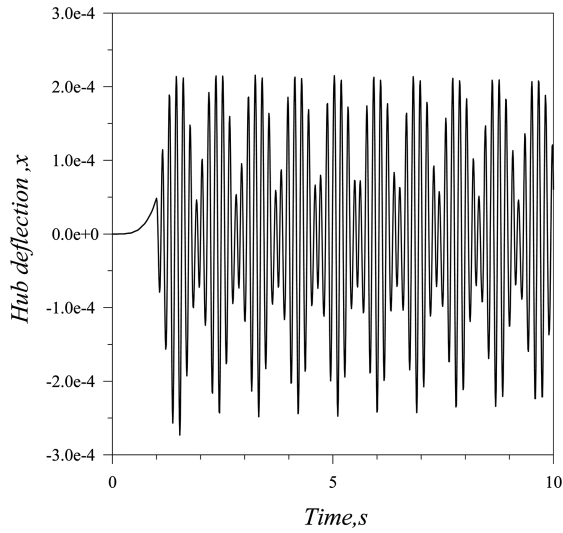


Fig. 16 Horizontal hub deflection for  $K_t = 10^6$ ,  $K_x = 10^5$ ,  $K_y = 10^4$  N/m and linear torque profile

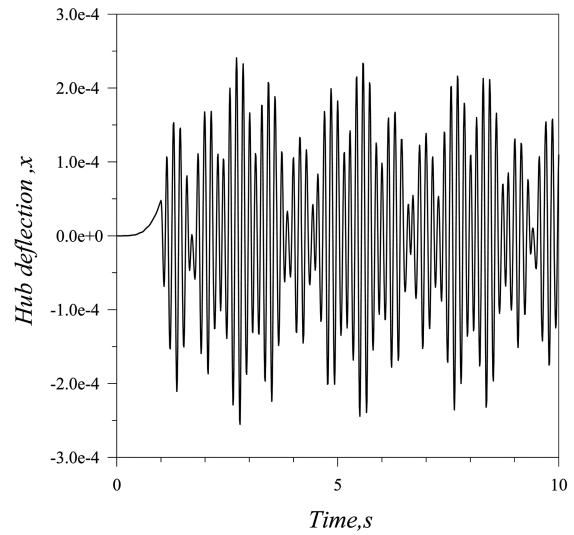


Fig. 17 Horizontal hub deflection for  $K_t = K_x = K_y = 10^5$  N/m and linear torque profile

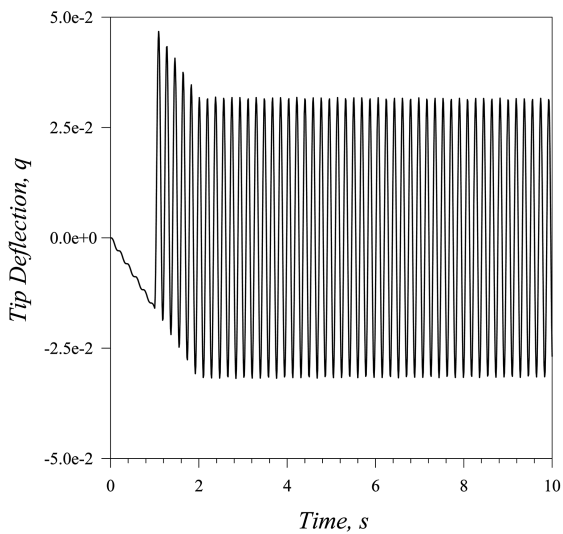


Fig. 18 Beam tip deflection for  $K_t = 10^4$ ,  $K_x = 10^2$ ,  $K_y = 10^2$  N/m and linear torque profile (first mode)

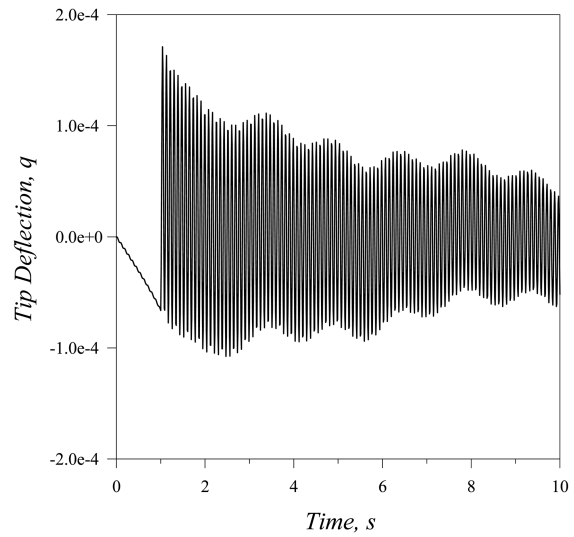


Fig. 19 Beam tip deflection for  $K_t = 10^4$ ,  $K_x = 10^2$ ,  $K_y = 10^2$  N/m and linear torque profile (second mode)

Results were obtained also for low values of stiffness,  $K_t = 10^4$ ,  $K_x = 10^3$  and  $K_y = 10^2$ , and presented in Figs 18-20, for the first three modes of the beam. Here the amplitude of the beam non-dimensional tip deflection of the first mode is relatively large when compared to those of the second and third modes. This indicates that the first mode of vibration is more important than the higher modes, because when exciting the system with a frequency close to the fundamental one, the amplitude of the first mode is higher and more dangerous than the other ones.

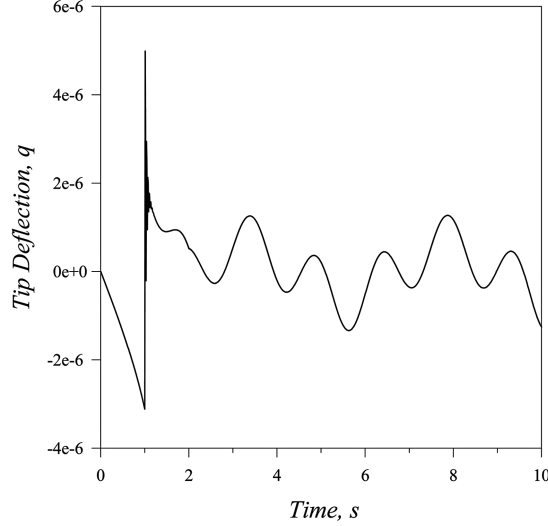


Fig. 20 Beam tip deflection for  $K_t = 10^4$ ,  $K_x = 10^2$ ,  $K_y = 10^2$  N/m and linear torque profile (third mode)

### 3.1 Reduced model

In certain situations, the system under consideration may get excited from its base, *i.e.* from the coordinated  $x$  and  $y$ . And this is a practical case when, for example, the system is excited from an unbalance force due to eccentricity ( $R$ ) in the driving motor which rotates at a speed ( $\Omega$ ). In such cases, the order of the system can be reduced and one can assume that

$$x = R \cos(\Omega t) \quad (28)$$

$$y = R \sin(\Omega t) \quad (29)$$

where  $R$  and  $\Omega$  are the excitation amplitude and frequency, respectively.

Upon substituting Eqs. (28) and (29) into the first two equations of the mathematical model, Eqs. (30) and (31), one obtains

$$2[\beta_1 + (\beta_2 - \beta_7)q^2 - \beta_8 q^4] \ddot{\theta} + 4(\beta_2 - \beta_7) \dot{\theta} q \dot{q} - 8\beta_8 \dot{\theta} q^3 \dot{q} + \beta_3 \ddot{q} + \Omega^2 R \{ [\beta_{10} q \cos \theta + (\beta_9 + \beta_{11}) \sin \theta] \cos(\Omega t) + [\beta_{10} q \sin \theta - (\beta_9 + \beta_{11}) \cos \theta] \sin(\Omega t) \} = 0 \quad (30)$$

$$2\beta_4 \ddot{q} + 2[\beta^2 \beta_5 + (\beta_7 - \beta_2) \dot{\theta}^2 + \beta^2 \beta_{14} S_t] q + 4[\beta^2 \beta_6 + \beta_8 \dot{\theta}^2 + \beta^2 \beta_{15} S_t] q^3 + \beta_3 \ddot{\theta} + \Omega^2 R \beta_{12} (\sin \theta \cos(\Omega t) - \cos \theta \sin(\Omega t)) = 0 \quad (31)$$

Eqs. (30) and (31), represent a reduced order mathematical model of the system under consideration. In order to select the right excitation frequencies, the linear natural frequencies of the hub-beam can be written in the form

$$\omega_n = \sqrt{\frac{2\beta^2 \beta_1 (2\beta_5 + \beta_{14} S_t)}{4\beta_1 \beta_4 - \beta_3^2}} \quad (32)$$

The values of the natural frequencies calculated for some values of  $K_t$ , of the beam-hub and for the first three modes are presented in Table 2.

Table 2 Beam-Hub natural frequencies

$k_t$	$\omega_{n1}$	$\omega_{n2}$	$\omega_{n3}$
$10^7$	35.22	77.08	212.47
$10^6$	35.19	77.00	212.25
$10^6$	35.19	77.00	212.25
$10^5$	34.99	76.22	210.17
$10^4$	33.05	70.28	196.27

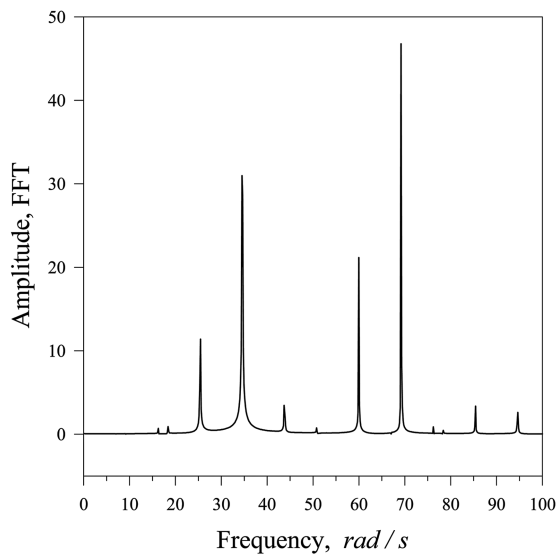


Fig. 21 Beam tip deflection spectrum (first mode) for  $R = 0.1$ ,  $\Omega = 30 \text{ rad/sec}$  and  $K_t = 10^4$

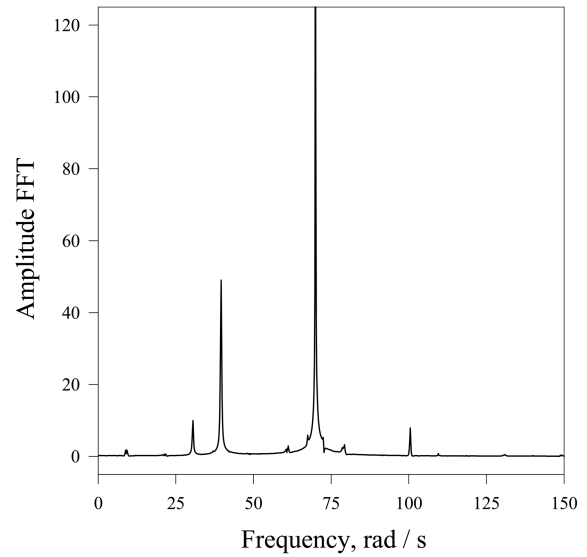


Fig. 22 Beam tip deflection spectrum (second mode) for  $R = 0.1$ ,  $\Omega = 35 \text{ rad/sec}$  and  $K_t = 10^4$

To have an idea about the system response under excitation from the base, results were obtained for different excitation frequencies and excitation amplitudes and for different modes of vibration.

In Fig. 21, the FFT of the beam tip deflection of the first mode is shown for  $K_t = 10^4$ ,  $\Omega = 30 \text{ rad/sec}$ ,  $R = 0.1$ . The spectrum shows frequencies with large amplitudes not only at the excitation frequencies but also at multiples of the excitation frequency, and this is due to the nonlinearities present in the system which can excite the sub and/or super harmonics of different orders.

The FFT of the beam tip deflections of the second mode is shown in Figs. 22 and 23 for the same parameters but with different excitation frequencies  $\Omega = 35 \text{ rad/sec}$ , and  $\Omega = 70 \text{ rad/sec}$  respectively.

The spectrum in Fig. 22 has, relatively, two peaks only at  $\Omega = 40, 70$ . While the results obtained in Fig. 23 show a spectrum that covers the whole frequency range. *i.e.* most of the frequencies and their sub and super harmonics are excited. A typical spectrum is obtained for the third mode, Fig. 24, *i.e.* one peak with high amplitude at the excitation frequency  $\Omega = 196 \text{ rad/sec}$ , this indicates that the natural frequencies calculated from Eq. (32) are approximate ones.

The natural frequencies of the beam-hub system depend on physical properties of the beam  $EI$ , beam mass per unit length  $\rho$ , Hub radius  $R_H$ , Hub mass  $M_H$  and torsional spring constant  $S_r$ . And this indicates that the system may lose its stability for certain combinations of physical parameters and this can be proved by calculating the equilibrium point of the beam-hub system and evaluating the Jacobian of the

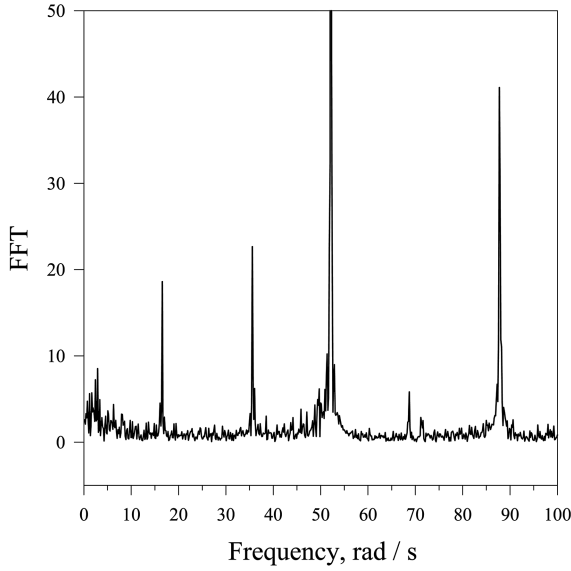


Fig. 23 Beam tip deflection spectrum (second mode) for  $R = 0.1$ ,  $\Omega = 70$  rad/sec and  $K_t = 10^4$

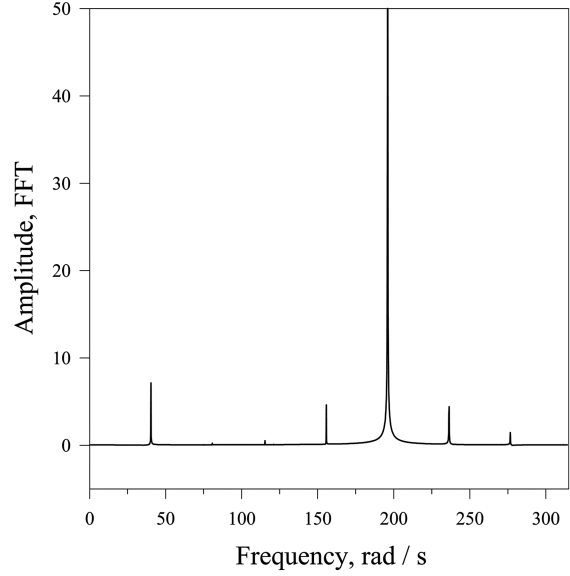


Fig. 24 Beam tip deflection spectrum (third mode) for  $R = 0.05$ ,  $\Omega = 196$  rad/sec and  $K_t = 10^4$

system., which can be obtained by firstly writing the system Eqs. (30 and 31) in a matrix form

$$\begin{bmatrix} 1 & 0 & 0 & 0 \\ 0 & 2(\beta_1 + (\beta_2 - \beta_7)q^2 - \beta_8q^4) & 0 & \beta_3 \\ 0 & 0 & 1 & 0 \\ 0 & \beta_3 & 0 & 2\beta_4 \end{bmatrix} \begin{Bmatrix} \dot{x}_1 \\ \dot{x}_2 \\ \dot{x}_3 \\ \dot{x}_4 \end{Bmatrix} = \begin{Bmatrix} x_2 \\ -4(\beta_2 - \beta_7)x_2x_3x_4 + 8\beta_8x_2x_3^2x_4 \\ x_4 \\ -4(\beta^2\beta_6 + \beta_8x_2^2)x_3^3 - 2(\beta^2\beta_5 + (\beta_7 - \beta_2)x_2^2)x_3 \end{Bmatrix} \quad (33)$$

where  $x_1 = \theta$ ,  $x_2 = \dot{\theta}$ ,  $x_3 = q$  and  $x_4 = \dot{q}$ . For simplicity, the system equations can be represented in the following matrix form

$$\mathbf{M}\dot{\mathbf{x}} = \mathbf{B} \quad (34)$$

where  $\mathbf{M}$  is the coefficient matrix and  $\dot{\mathbf{x}}$  is the state space vector which contains  $\dot{x}_1$ ,  $\dot{x}_2$ ,  $\dot{x}_3$  and  $\dot{x}_4$ .

The equilibrium points of the system can be calculated by setting  $\dot{\mathbf{x}} = \mathbf{M}^{-1}\mathbf{B} = \mathbf{0}$  and solving for  $x_1$ ,  $x_2$ ,  $x_3$  and  $x_4$ , such that

$$\begin{aligned} x_2 &= 0 \\ x_4 &= 0 \\ x_3^2 &= \frac{-(\beta_7 - \beta_2) \pm \sqrt{(\beta_7 - \beta_2)^2 + 4\beta_1\beta_8}}{2\beta_8} \end{aligned} \quad (35)$$

It worth mentioning here that  $x_1$  doesnot appear in Eq. (33), because the degree of freedom  $\theta$  doesnot appear explicitly in system Eqs. (22-25), and consequently the solutions obtained for the singular points  $(x_2, x_3, x_4)$  are valid for any value of  $x_1$ .

The jacobian of the system can be written in the form

Table 3 Singular points and eigenvalues of the system Jacobian

No.	Singular Point	Eigenvalues			
		$\lambda_1$	$\lambda_2$	$\lambda_3$	$\lambda_4$
1	-1.22827	(0,25.3588)	(0,42.5217)	(0,0)	(0,0)
2	-2.17512	(0,-25.3588)	(0,-42.5217)	(0,0)	(0,0)

$$\mathbf{J} = \frac{\partial}{\partial \mathbf{x}_u} (\mathbf{M}^{-1} \mathbf{B}) \quad (36)$$

The stability of the system near the equilibrium points can be examined by evaluating the eigenvalues of the Jacobian matrix  $\mathbf{J}$ .

For different values of  $S_r$ , the eigen values of the Jacobian matrix were calculated and all them were a pair of complex conjugate and this indicate that the sytem might undegor a Hopf Bifurcation when the eigenvalues crosses the imaginary axis and their real parts change sign, i.e positive values. As an example, for  $K_r = 10^6$  the values of the singular points and the corresponding eigenvalues are given in the Table 3.

As indicated previously in the results obtained in Fig. 15, the angular system loses its stability, and the angular position continue to increase even after the end of the maneuver. This indicate that further analysis is needed to study the exact nonlinear natural frequencies and stability conditions of the system, which is beyond the scope of the present work.

#### 4. Conclusions

The nonlinear dynamic model and behavior of a rotating beam with flexible root attached to a rotating hub with elastic foundation is developed and studied. The coupled nonlinear equations of motion were obtained using the Lagrangian dynamics and the assumed mode method. The numerical simulations have shown that the root flexibility and hub stiffness have a noticeable effect on beam tip deflection, hub angular position and hub horizontal and vertical displacements.

Results of the numerical simulations have shown some damping effect and hub may not reach its prescribed angular position due to the nonlinear interaction and energy transfer between different degrees of freedom. It can be concluded that the stiffness of the hub has a critical value below which the hub has a destabilizing effect of the dynamic behavior of the system. In addition and in light of the presented results and analysis, and as indicated by the numerical simulations, the beam-hub system may loses its stability when; 1) the frequency of the input torque and/or the excitation frequency is close to one of the beam-hub natural frequencies, or when the system operates under certain conditions and/or with a combination physical parameters. To have a clear and global picture on the qualitative analysis of the dynamical behavior stability, further investigations are highly recommended.

#### Aknowldgements

The author acknowledge the support of the University of Jordan. This research was conducted during a sabbatical leave for the accademic year 2005/2006 granted by the University of Jordan.

## References

- Al-bedoor, B.O. and Hamdan, M.N. (2001), "Geometrically non-linear dynamic model of a rotating flexible arm", *J. Sound Vib.*, **240**, 59-72.
- Al-bedoor, B.O. and Al-qaisia, A.A. (2002), "Analysis of rotating blade forced vibration due to torsional excitation using the method of harmonic balance", *Proceedings of ASME 2002 Pressure Vessels & Piping Conference*, Vancouver, Canada, August.
- Al-bedoor, B.O. and A.A. Al-qaisia (2005), "Stability analysis of rotating blade bending vibration due to torsional excitation", *J. Sound Vib.*, **282**, 1065-1083.
- Al-qaisia, A.A. (2002), "Nonlinear free vibration of a rotating beam carrying a tip mass with rotary inertia", *Proceedings of ASME 2002 Pressure Vessels & Piping Conference*, Vancouver, Canada, August.
- Al-qaisia, A.A. (2003), "Effect of Fluid Mass on Non-Linear Natural Frequencies of a Rotating Beam", *Proceedings of ASME 2003 Pressure Vessels & Piping Conference*, Cleveland, Ohio, July.
- Al-qaisia, A.A. (2004), "Non-linear dynamics of a rotating beam clamped with an attachment angle and carrying an inertia element", *Arab. J. Sci. Eng.*, **29**(1C), 81-97.
- A.A. Al-qaisia and B.O. Al-bedoor (2005), "Evaluation of different methods for the consideration of the effect of rotation on the stiffening of rotating beams", *J. Sound Vib.*, **280**, 531-553.
- Baerjee, J.R. (2000), "Free vibration of centrifugally stiffened uniform tapered beams using the dynamic stiffness method", *J. Sound Vib.*, **233**, 857-875.
- Baruh, H. and Tadikonda, S.K. (1989), "Issues in the dynamics and control of flexible robot manipulators", *J. Guidance*, **12**, 659-671.
- Bazoune, A., Khulief, Y.A. and Stephen, N.G. (1999), "Further results for modal characteristics of rotating tapered timoshenko beams", *J. Sound Vib.*, **219**, 157-174.
- El-absy, H., Shabana, A.A. and Shabana, A.A. (1997), "Geometric stiffness and stability of rigid body modes", *J. Sound Vib.*, **207**, 465-496.
- Haering, W.J., Ryan, R.R. and Scott, R.A. (1994), "A new flexible body dynamic formulation for beam structures undergoing large overall motion", *J. Guid. Control Dyn.*, **17**, 76-83.
- Hamdan, M.N. and Al-bedoor, B.O. (2001), "Non-linear free vibrations of a rotating flexible arm", *J. Sound Vib.*, **242**, 839-853.
- Hoa, S.V. (1979), "Vibration of a rotating beam with tip mass", *J. Sound Vib.*, **67**, 369-381.
- Lee, H.P. (1993), "Vibration on an inclined rotating cantilever beam with tip mass", *ASME J. Vib. Acoustics*, **115**, 241-245.
- Lin, S.C. and Hsiao, K.M. (2001), "Vibration analysis of a rotating timoshenko beam", *J. Sound Vib.*, **240**, 303-322.
- Mitchel, T.P. and Bruch, J.C. (1988), "Free vibrations of a flexible arm attached to a compliant finite hub", *ASME J. Vib., Acoustics*, **110**, 118-120.
- Mulmule, S., Singh, G. and Venkateswara, R. (1993), "Flexural vibrations of rotating tapered timoshenko beams", *J. Sound Vib.*, **160**, 372-377.
- Pohit, G., Mallik, A.K. and Venkatesan, C. (1999), "Free out-of-plane vibrations of a rotating beam with non-linear elastomeric constraints", *J. Sound Vib.*, **220**, 1-25.
- Tadikonda, S.K. and Chang, H.T. (1995), "On the geometric stiffness in flexible multibody dynamics", *ASME J. Vib. Acoustics*, **117**, 452-461.
- Yigit, A.S., Ulsoy, A.G. and Scott, R.A. (1990), "Dynamics of a radially rotating beam with impact, Part 1: theoretical and computational model", *ASME J. Vib. Acoustics*, **112**, 65-70.
- Yoo, H.H. and Shin, S.H. (1998), "Vibration Analysis of Rotating Cantilever Beams", *J. Sound Vib.*, **212**, 807-828.